Optimisation of a High-Efficiency Solar-Driven Organic Rankine Cycle for Applications in the Built Environment

Alba Ramos[a], Maria Anna Chatzopoulou[b], James Freeman[c], Christos N. Markides[d]

[a] Clean Energy Processes (CEP) Laboratory, Department of Chemical Engineering, Imperial College London, London SW7 2AZ, UK, a.ramos-cabal@imperial.ac.uk (CA)
[b] Clean Energy Processes (CEP) Laboratory, Department of Chemical Engineering, Imperial College London, London SW7 2AZ, UK, maria-anna.chatzopoulou11@imperial.ac.uk (CA)
[c] Clean Energy Processes (CEP) Laboratory, Department of Chemical Engineering, Imperial College London, London SW7 2AZ, UK, j.freeman12@imperial.ac.uk
[d] Clean Energy Processes (CEP) Laboratory, Department of Chemical Engineering, Imperial College London, London SW7 2AZ, UK, c.markides@imperial.ac.uk

Abstract:

Recent years have seen a strong increase in the uptake of solar technologies in the built environment. In combined heat and power (CHP) or cogeneration systems, the thermodynamic and economic 'value' of the electrical output is usually considered to be greater than that of (an equivalent) thermal output, and therefore the prioritisation of the electrical output in terms of system-level optimisation has been driving much of the research, innovation and technology development in this area. In this work, the potential of a solar CHP technology based on an organic Rankine cycle (ORC) engine is investigated. We present thermodynamic models developed for different collectors, including flat-plate collectors (FPC) and evacuated-tube collectors (ETC) coupled with a non-recuperative sub-critical ORC architecture to deliver power and hot water by using thermal energy rejected from the engine. Results from dynamic 3-D simulations of the solar collectors together with a thermal energy storage (TES) tank are presented. TES offers an important buffering capability during periods of intermittent solar radiation, as well as the potential for demand-side management (DSM). Results are presented of an optimisation analysis to identify the most suitable working fluids for the ORC unit, in which the configuration and operational constraints of the collector array are taken into account. The most suitable working fluids (R245fa and R1233zd) are then chosen for a whole-system optimisation performed in a southern European climate. The system configuration with an ETC array is found to be best-suited for electricity prioritisation, delivering an electrical output of 3,605 kWh/yr from a 60 m^2 array. In addition, the system supplies 13,175 kWh/yr in the form of domestic hot water, which is equivalent to more than 6 times the average annual household demand. A brief cost analysis and comparison with photovoltaic (PV) systems are also performed.

Keywords:

Solar energy; Organic Rankine cycle; Dynamic modelling; Optimisation; Energy efficiency.

1. Introduction

The 18% adoption rate of renewable power (not including hydro) experienced in 2015 was the highest annual growth rate ever recorded [1]. This can be attributed to supportive government policies, strong end-user demand, and sharp cost reductions on the technology side leading to improved system cost-effectiveness. The global investment in renewables also climbed to a record level in 2015 [1,2], such that to-date, renewable sources supply about 14% of the world's total energy consumption [3].

The uptake of solar energy technologies in the built environment, including solar photovoltaic (PV) systems, solar hot-water and space heating systems and hybrid combined PV-thermal (PV-T) systems, has increased in-line with the trends described above [4]. The thermodynamic and economic 'value' of renewable electricity is typically considered to be greater than that of (an equivalent) thermal output, and this has been driving much of the research, innovation and technology development in the area of solar electricity generation. The most established technology for solar power generation are PV systems, which directly convert solar irradiation into electricity. PV module (panel) efficiencies are in the range 14-17%, for cell efficiencies between 18-21%. These numbers

have only increased by 3-6% in the last 10 years with a further 2-4% increment expected by 2020 [5]. Higher-efficiency concentration PV modules (CPV) are also commercially available, but these are and are expected to remain economically uncompetitive in the short term [6]. For PV systems, when generation is greater than the demand, the electricity can be stored (typically in batteries) or fed to the grid (except in isolated/off-grid systems). However, battery storage for PV is expensive with current best-case cost estimates in the region of 125-170 GBP/kWh [7], while PV without storage is of limited use for demand-side management (DSM) due to the mismatch between peak solar availability (around mid-day) and peak electrical demand (typically during winter evening hours).

Solar thermal systems, on the other hand, use collectors to convert solar radiation into a thermal output (enthalpy flow). This can be stored at a lower-cost and with reduced losses in thermal energy storage (TES) media, for later use in a wide range of services including hot-water provision, space or process heating, or even power generation, refrigeration or water desalination. In domestic hot-water (DHW) applications, solar collectors are usually coupled to a hot water tank for TES provision; either directly or indirectly via a heat exchanger and separate fluid loop. Domestic solar thermal systems are well-established and commercially mature, with collector design-point efficiencies often exceeding 60%. A wide range of stationary non-concentrating (low-concentration) collector designs are available for urban applications (e.g. flat-plate collectors, evacuated-tube direct-flow collectors and heat pipes). The selection of a particular collector design can be matched to the application and the required temperature of operation, which may vary typically between 70 and 220 ºC [8].

The organic Rankine cycle (ORC) is a thermodynamic cycle that uses an organic substance as the working fluid, and is particularly suitable for the conversion of low-/medium-grade (i.e. temperature) heat to electrical power in small-/medium-scale systems. The selection of a suitable working-fluid allows ORC engines to operate efficiently with low-to-medium temperature heat sources, including geothermal energy [9], process waste heat [10,11] and non-concentrating (low-cost) solar thermal collectors [12]. Due to their suitability in small-scale applications, considerable attention has been given to the development of ORC systems for distributed power generation, and in combined heat and power and poly-generation applications for domestic and commercial buildings [12].

In this work, we investigate the electrical and thermal performance of a solar-combined heat and power (CHP) system based on non-concentrating solar collectors and an ORC engine. Unlike previous studies that focus on the optimisation of the ORC subsystem, this study also considers the design parameters of the solar collector in order to optimise the overall system design and operation.

2. Modelling framework and methodology

In this work, the potential of solar-driven ORC systems for providing heat and power is investigated, focusing on applications in the built environment. Thermodynamic models for the different technologies are developed, and the electrical and thermal outputs of alternative system configurations are evaluated and compared. The configurations considered in this study include two types of solar collectors coupled to a subcritical non-recuperative ORC engine: i) a FPC array; and ii) an ETC array. In both cases, the overall system is optimised in order to maximise the electrical output.

The percentage of roof area available for the installation of solar collectors in a single-residence dwelling is assumed to be about 50% of the household area [13]. In the present case study, this is equivalent to an available area of 60 m^2 (average household size of 120 m^2, 4-6 people). In Fig. 1, a schematic illustration is presented of the two system configurations studied in this work. In both configurations, the aim is to maximise the overall electrical output. At the same time, the system design allows excess heat from the ORC engine to be utilised for hot-water heating (DHW provision). To achieve this, the heat-transfer fluid temperature at the ORC evaporator outlet is set to be between 55 and 60 ºC, which is a typical temperature range for DHW services [14].

To take advantage of the TES subsystem, the ORC unit will be running for a period of the day that does not necessarily correspond to the hours of solar availability, but rather to the period of peak electricity demand in Europe (which is typically from 18-19 to 22-23 h) [17]. This operating strategy

is chosen to reduce the stress on the electricity grid during hours of peak demand, and is intended as part of a wider DSM strategy to reduce the required capacity of so-called peaking power plants.

The modelling was conducted in the MATLAB and TRNSYS software environments [15]. An experimentally validated 3-D MATLAB model was used for the modelling of the FPCs, and a model developed in TRNSYS was used for the ETCs (Type 71). For the ORC unit performance predictions, an in-house MATLAB code for non-recuperative ORC engines was used, which was validated against available data in the literature. The individual subsystem models were coupled together to form the different configurations presented in Fig. 1. The dynamic response of the complete system (solar collectors and ORC engine) to time-varying climate data was studied in TRNSYS. The solar thermal collectors and the ORC unit size, along with the respective working fluids and key system operating conditions (pressures, temperatures, flow rates) were optimised so that the electrical power output is maximised. TRNSYS models were then used to obtain the hourly and daily performance results of the complete system for different seasonal weather inputs. The analysis workflow is as follows:

- Firstly, the thermodynamic models of the solar collectors and ORC engine are developed (Section 3), based on which dynamic simulations are conducted for different solar collectors leading to final collector designs based on which performance curves are obtained (Section 4).
- Optimisation of the complete system of the ORC engine and the solar collectors is conducted aimed at identifying operating conditions for which the power output is maximised (Section 5).
- Hourly dynamic simulations of the optimised system configurations are then performed to complete the system sizing (Section 6).
- An economic analysis of the optimised configurations is conducted (Section 7), and finally, important conclusions from the present work are given (Section 8).

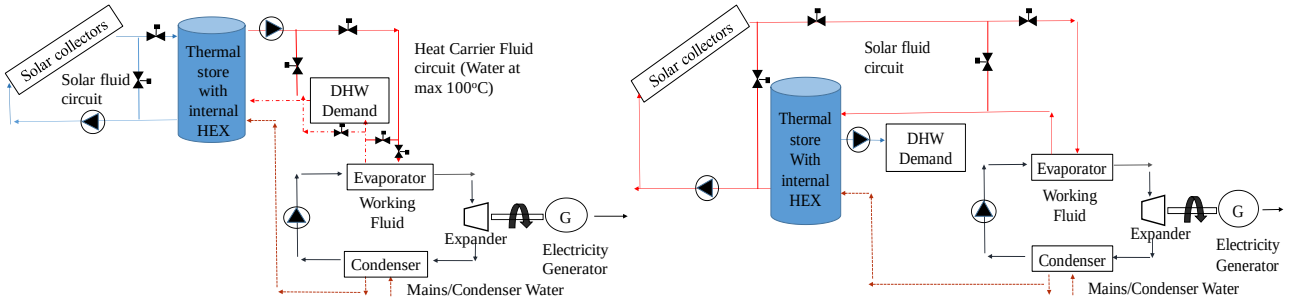

Fig. 1. Solar-driven ORC unit within the two studied system configurations based on: a) flat-plate collectors and b) evacuated-tube collectors.

3. Thermodynamic models

3.1. Solar thermal collectors

3.1.1 Flat-plate collectors (FPCs)

A 3-D solar-thermal collector model, developed in MATLAB, is used for the modelling of the FPC. The experimentally validated model, developed originally for the modelling of hybrid PV-thermal (PV-T) collectors and presented in detail in Guarracino et. al [16], has been modified in the present study for the modelling of sheet-and-tube water collectors. The numerical model is used to solve an energy balance by taking into account the convective and radiative losses from the collector's top surface and the optical losses due to reflection. For a given set of weather conditions and a known inlet temperature and fluid flow-rate, the fluid outlet temperature is obtained from the energy balance equation, which in turn allows the instantaneous thermal efficiency $\boldsymbol{\eta_{TH}}$ of the collector to be calculated as indicated in Eq. (1), where $\boldsymbol{\dot{m}}$ is the fluid mass flow-rate, $\boldsymbol{c_f}$ the specific heat of the fluid, $\boldsymbol{T_{in}}$ and $\boldsymbol{T_{out}}$ are the collector fluid temperatures at the inlet and outlet, $\boldsymbol{G}$ is the solar irradiance and

A is the area of the collector, such that the numerator and denominator correspond to the collector output thermal energy (rate) and the available incident solar power, respectively:

$$\eta_{\mathrm{TH}} = \frac{\dot{m} c_{\mathrm{f}} (T_{\mathrm{in}} - T_{\mathrm{out}})}{GA} . \quad (1)$$

The model also allows important design parameters to be varied, including the number of glass cover layers (glazing), the materials used for the glass cover and thermal absorber, the spacing between the tubes and the fluid mass flow-rate. A schematic diagram of the FPC construction is shown in Fig. 2a.

3.1.2 Evacuated-tube collectors (ETCs)

A TRNSYS component (Type 71) has been chosen for the modelling of the ETC array. This model is used to predict the thermal performance of a variety of ETC types as a function of the fluid/collector temperature, ambient temperature and solar irradiance. The collector efficiency is calculated as a quadratic function of the reduced temperature T_{red}, using the empirical coefficients η_0, c_1 and c_2 obtained through steady-state performance testing of real collectors according to standard EN 12975. The reduced temperature T_{red} is defined as the difference between the average collector temperature T_{m} and the ambient air temperature T_{amb}, divided by the solar irradiance:

$$\eta_{\mathrm{TH}} = \eta_0 - c_1 T_{\mathrm{red}} - c_2 G {T_{\mathrm{red}}}^2 ; \quad (2)$$

$$T_{\mathrm{red}} = \frac{(T_{\mathrm{m}} - T_{\mathrm{amb}})}{G} . \quad (3)$$

The effects of non-perpendicular solar incidence angle are modelled using a bi-axial incidence angle modifier (IAM) data file. For a given set of climate conditions at each time interval, the model calculates the useful energy output of the solar collector and the resulting increase in the temperature of the circulating fluid. The ETC model chosen for this study is based on the empirical efficiency curve coefficients of a heat pipe collector design, and is shown in Fig. 2b.

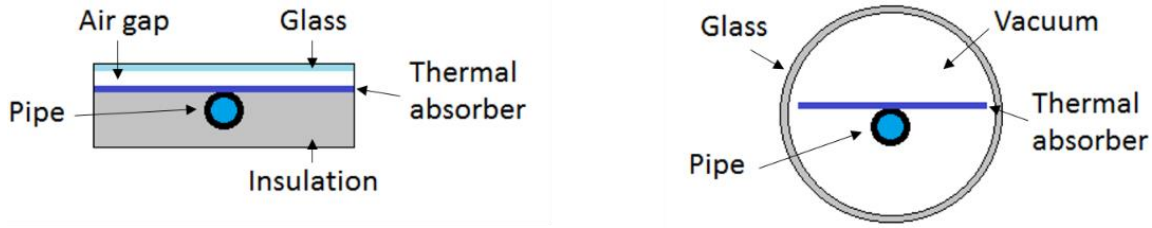

(a) (b)

Fig. 2. Schematic diagram showing the two types of collector modelled in the study: (a) flat-plate solar thermal collector and (b) evacuated-tube collector.

3.2. Organic Rankine cycle (ORC) engine

A steady-state model of an ORC engine has been developed in MATLAB, and validated against available ORC operating data in the literature. This model is used to optimise the ORC system design for maximum power output. The thermodynamic model of the cycle considers the processes illustrated on the *T-s* diagram in Fig. 3. Specifically, States 1-2 correspond to the pumping process of the organic fluid, States 2-3 to the heat addition process, States 3-4 to the expansion process through the turbine/expander, where work is generated, and States 4-1 to the heat rejection process from the cycle. Also shown are Process 5-6, which demonstrates the increase in the enthalpy of the condenser cooling-water stream as this absorbs the heat rejected from the cycle, and Process 7-8, which demonstrates the decrease in enthalpy experienced by the heat-transfer (source) fluid, as this provides heat to the cycle. Mass and energy balance equations are applied to each system component, followed by an exergy analysis. The model results provide estimates of all the operating points illustrated in Fig. 3, along with the ORC unit power output, thermal and exergy efficiencies. The interested reader can find further details on the thermodynamic model of the ORC system in Chatzopoulou et al. [11].

3.3. Thermal storage tank

A TRNSYS component (Type 534) has been considered [15] for the model of the TES vessel, which is a stratified hot-water tank featuring an immersed heat exchanger. The water tank is modelled by assuming that it consists of N fully-mixed volume segments. In the present case, N has been set to 4. In addition, the tank includes an auxiliary heater to reach the minimum end-use temperature requirements that will vary according to each configuration (see Sections 4 and 5).

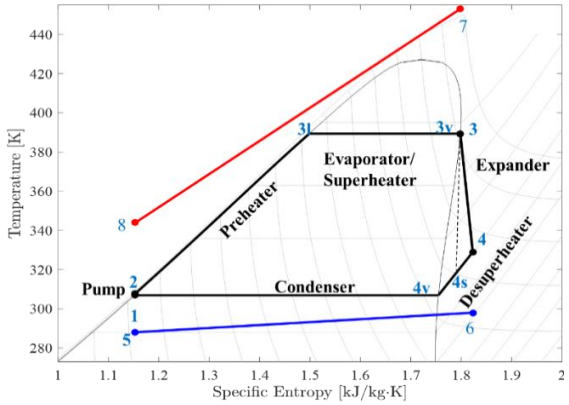

Fig. 3. Non-recuperative, non-superheated sub-critical ORC on a T-s diagram.

4. Modelling and design of solar thermal collectors

First, preliminary simulations using the solar collector models presented in Section 3.1 are performed, aimed at obtaining collector-array sizes, fluid flow-rates and efficiency curves over a range of representative irradiation conditions and solar fluid temperatures. This is achieved by imposing a number of operational constraints that account for: i) the ORC temperature requirements; and ii) the available roof area to be covered with collectors. Dynamic simulations of the solar collector array (without the ORC subsystem) are performed in TRNSYS [15] to obtain the optimal configuration settings (array area, mass flow rate, etc.) for use in the full solar-ORC system optimisation. As mentioned earlier, the location of the system has a significant impact on the selection, configuration and operation of the collector array, as the available irradiance will influence the performance of the collector. Athens (Greece) is the selected location in this work for modelling both types of collectors. However, results can be extrapolated to similar Southern locations as explained in Section 6.

4.1. Flat-plate collector (FPC) performance

This collector will be coupled with the ORC unit by means of a thermal storage unit as indicated in in Fig. 1a. For this system configuration, a single glazed sheet-and-tube collector is designed. The area of a single collector is 1.19 m^2 (based on a width of 1.56 m and length of 0.76 m), consisting of 14 riser tubes, with a tube diameter of 6.8 mm. The absorber thermal conductivity is 310 W/(m·K) and the absorptivity of the front surface is 0.9. The fluid considered is a water-glycol mixture and the total flow rate per collector is constrained within the range 0.01-0.03 kg/s. A volume of 150 L is chosen for the hot water tank, which corresponds to the standard household size in Europe [13].

As noted above, a number of feasibility constraints are applied to the operational settings for the whole-system optimisation model. These are as follows:

1) The desired temperature difference between the inlet and outlet of the collector array is 50-80 ºC and the outlet temperature from the thermal store to the ORC unit is 80-100 ºC, for average irradiance conditions during daylight hours.
2) The total mass flow-rate in the solar collector array is equal to that of the ORC heat source.

In order to achieve the first constraint, in-series connections of one or more collector modules is permitted. This means that the fluid exiting one collector enters the following one, so that the mean temperature of the collectors increases from the first module to the last module, while the flow rate through each individual collector module is equal to the total flow rate in each branch. In addition, to

meet the second constraint, parallel branches of collector modules are allowed so that the overall flow rate in the entire array can be increased. The flow rate on the heat-source side of the ORC evaporator can vary between 0.01 and 0.09 kg/s, with a maximum of three branches arranged in parallel. More details on the ORC design constraints are provided in Section 5.

For the selected location, Athens, the average irradiance amounts to 198 W/m^2 with an average of 11 sunny hours per day. During daylight hours, the average irradiance is 432 W/m^2, and for 60% of the sunny hours it is above 600 W/m^2. These results have been obtained from analysis of hourly data covering a period of one year, extracted from the Meteonorm database [17] for use in TRNSYS.

From the dynamic simulations, the FPC design configuration that fulfils the constraints described in Eqs. (1) and (2) for more than 60% of the annual daylight hours results in the expression for the collector efficiency given by:

$$\eta_{\mathrm{TH}} = 0.6483 - 4.6948\, T_{\mathrm{red}} \,. \quad (4)$$

4.2. Evacuated-tube collector (ETC) performance

The ETC array interfaces with the ORC engine via a thermal storage vessel as indicated in Fig. 1b. Both models have been presented in Section 3. Performance curve coefficients for the commercial ETC Gasokol vacuTube65/20 have been used [18]. The heat transfer fluid is taken as thermal oil Therminol 66 [19] and the mass flow-rate is constrained to within the range 0.017-0.069 kg/s. The area of a single collector module is 1.5 m^2 and the hot water tank volume is 150 L as before.

The following constraints are applied to the operational settings of whole-system optimisation model:

1) The desired temperature difference between the inlet and outlet of the collector array is 140-160 ºC and the outlet temperature from the thermal store to the ORC unit is 180-200 ºC, for average irradiance conditions during daylight hours.
2) The total mass flow-rate in the solar collector array is equal to that of the ORC heat source.

Again, collector modules are permitted to be connected in series and/or parallel configurations in order to meet both constraints. In this case, the resulting range for the ORC heat source flow-rate is 0.017-0.300 kg/s. For the selected location, Athens, the efficiency curve of the ETC selected to meet the above constraints for more than 60% of the annual daylight hours is described by:

$$\eta_{\mathrm{TH}} = 0.710 - 1.25\, T_{\mathrm{red}} - 0.045\, G\, {T_{\mathrm{red}}}^2 \,. \quad (5)$$

5. Solar-driven ORC system optimisation

5.1 Optimisation problem definition

A typical optimisation problem includes an objective function $Z(\vec{X})$ that we seek to minimise/maximise, subject to some constraints, where $\vec{X}$ is a vector containing all the decision variables that the optimiser can vary. In this work $\vec{X}$ includes six variables: i) evaporator pressure (P_{evap}); ii) condenser pressure (P_{con}); iii) superheating degree (SHD); iv) working fluid flow-rate ($\dot{m}_{\mathrm{wf}}$); v) HEX pinch point (PP); vi) expander volume ratio (r_{exp}); vii) heat source flow rate ($\dot{m}_{\mathrm{hs}}$); and viii) heat source inlet temperature to the ORC unit ($T_{\mathrm{hs,in}}$). For each of these decision variables a respective range of feasible values has been selected. A case in the point, $\dot{m}_{\mathrm{hs}}$ is constrained to up to 0.09 kg/s for the FPC array and up to 1.79 kg/s for the ETC array. The key problem constraints are summarised in Eqs. (6) to (12) (non-exhaustive list).

Maximise: $$\{\dot{W}_{\mathrm{net}}\} = Z(P_{\mathrm{evap}}, P_{\mathrm{con}}, \dot{m}_{\mathrm{wf}}, SHD, PP, r_{\mathrm{exp}}, \dot{m}_{\mathrm{hs}}, T_{\mathrm{hs,in}}) \quad (6)$$

Subject to: $$P_{\mathrm{con}} < P_{\mathrm{evap}} < P_{\mathrm{crit}} \quad (7)$$

$$PP_{\mathrm{min}} \leq PP \quad (8)$$

$$\frac{P_{\mathrm{evap}}}{P_{\mathrm{con}}} \leq {r_{\mathrm{exp}}}^{\gamma} \quad (9)$$

$$A_{\mathrm{col}} \leq A_{\mathrm{max}} \quad (10)$$

$$T_{\mathrm{lim}} \leq T_{\mathrm{hs,out}} \quad (11)$$

In this set of equations, Eq. (7) ensures that the operating pressure levels in the system remain below the critical pressure, Eq. (8) ensures that the minimum pinch temperature difference PP is not violated, Eq. (9) ensures that the expander operates isentropically, Eq. (10) limits the maximum collector area, and Eq. (11) constrains the heat-transfer fluid temperature leaving the ORC system.

Furthermore, the expander technology selected is that of positive-displacement reciprocating machines, since this allows a wide range of operating pressure ratios. Finally, a reciprocating fixed-speed pump is selected as the pressurisation pump for the ORC subsystem.

5.2 Optimisation results

The solar-ORC system has been optimised for six working fluids, namely R245fa, R1233zd, R152a, R1234ze, R1234yf, butane and pentane, which were selected based on their good thermodynamic performance and good environmental behaviour. The power output of the optimum ORC unit when coupled with a FPC array is shown in Fig. 4a for all working fluids. R245fa and R1233zd have the highest power outputs, reaching 460 W, followed by R152a and butane with 451 W. Pentane exhibits the lowest power output of 303 W. An examination of the performance of the solar-ORC systems in terms of power output shows that the poorer-performing working-fluids, such as pentane, result in lower pressure ratios over the expander ($r_{\text{exp}} \approx 2$) compared to the better-performing working-fluids such as R1233zd ($r_{\text{exp}} \approx 3.5$), as expected. The ORC thermal efficiency peaks at 5.5% for R245fa, with a FPC efficiency close to 30%. There is no significant variation in the efficiency of the collectors and the ORC among the working fluids investigated, because the optimum solar fluid temperatures leaving/entering the ORC are almost identical for all fluids, and equal to 55-60 ºC and 95-100 ºC respectively.

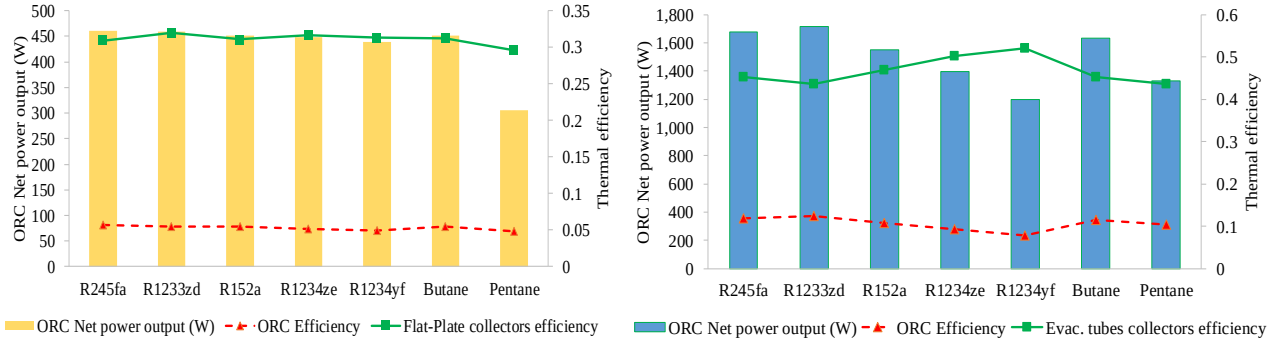

(a) (b)

Fig. 4. Solar-ORC system performance with: (a) FPC and (b) ETC, for I_{sol} = 600 W/m^2.

The performance of the solar-ORC system with an ETC array is presented in Fig. 4b. The power output obtained is significantly higher than the FPC-system equivalents, reaching a peak of 1,720 W for R1233zd, and 1,680 W for R245fa and butane. The higher power output is achieved: i) due to the higher solar fluid temperature exiting the collector array, which in this case corresponds to 150-200 ºC; and ii) due to the higher allowable solar-fluid mass flow-rate (see also Section 5.1). This results in an ORC efficiency in the range of 8-13%, while the collector efficiency varies between 44-52%. It is worth noting that for fluids such as R1234ze and R1234yf, the collector efficiency is the highest, above 50%, because the optimal temperature of the solar fluid leaving the collector is 150-160 ºC, which reduces the mean temperature of (and thus losses from) the collector. However, the lower heat-source temperature results in lower ORC power outputs and thermal efficiencies. In both systems, it was originally assumed that the optimiser would seek to maximise the heat source side ΔT and the flow rate simultaneously, in order to increase the thermal input to the ORC and thus the net power output. However, this was not possible without violating the pinch point in the evaporator, and without reducing dramatically the collector efficiency. Therefore, in all optimum cycles obtained, the flow rate of the collector configuration selected is close to the minimum values, with the ΔT being restricted by the pinch point. Additionally, the collector area requirements for both configurations are equal to the maximum allowable (60 m^2). This is due to the fact that multiple collectors connected in series are required, to achieve the elevated heat source temperature for the ORC unit. Finally, it is evident that the higher the heat-transfer fluid temperature, the higher the ORC unit power output.

6. System design for the optimised cycles

6.1 Solar-thermal ORC combined system sizing results

Key to the performance and financial viability of ORC units is the individual components selection and sizing. In this work, the evaporator heat exchanger (HEX) has been modelled by splitting the HEX into three distinct zones: i) a pre-heating zone with the organic fluid in the liquid phase; ii) an evaporating zone with the organic undergoing phase change; and iii) a superheating zone with the organic fluid in the vapour phase. Within each zone, further spatial discretisation is performed (dividing the HEX length into n segments). This allows the detailed calculation of local heat transfer coefficients (HTCs) in each segment along the length of the HEX, capturing the variations occurring during the phase change. Once the local HTCs are evaluated, the HEX size has been calculated using the Logarithmic Mean Temperature Difference (LMTD) method [20]. A similar approach has been applied to the condenser, which is divided into two zones: i) a desuperheating section, with organic fluid in vapour phase; and ii) a condensing section, with organic fluid in a two-phase state. Both HEXs are of a tube-in-tube construction, due to the low cost of such designs.

For the calculation of the HEX surface area requirements, the HTCs have been estimated based on Nusselt number correlations, using the Dittus-Bolter correlation in the single-phase zones [20], the correlations of Dobson [21] and Zuber [22] in the evaporating two-phase zones, and the correlation of Shah [23] in the condensing zones. Resulting HEX sizes for the examined working-fluids are shown in Fig. 6. With reference to this figure, the ETC-based system generally requires higher HEX surface areas, than the FPC system. This is in line with the higher power output achieved by the former, which results in larger component requirements. The FPC-based system has larger condenser area requirements than evaporator requirements, whereas in the EPC system this is reversed due to the high area requirements of the preheating zone for those cycles.

For R1234ze in Fig. 6a (FPC) the area requirements peak at approximately 1 m^2, which is mainly attributed to the size of the desuperheater for this fluid; the optimal cycle with R1234ze has a high superheating degree, which together with the higher working-fluid flow rate leads to a high desuperheating load and size. The HTC achieved in the vapour only zone is lower than the respective ones in the two-phase or liquid only, resulting in high area requirements for the desuperheater. The results for the ETC-based system in Fig. 6b indicate that the high heat-source temperatures achieved with this type of collector allow the optimum evaporating pressure to approach the critical values of the working fluids, such that the contribution of latent heat during phase change is a relatively small, and the preheating load is large. The HTCs obtained in the preheating area are, however, lower than the respective ones during phase change, resulting in high surface-area requirements.

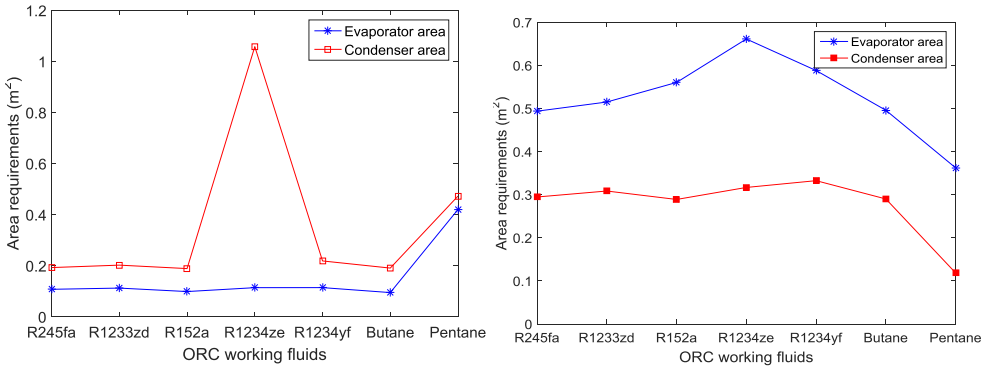

Fig. 6. HEX sizes for solar-ORC system with: (a) FPC and (b) ETC, for I_{sol} = 600 W/m^2

Furthermore, from the optimisation results we can obtain the size of the solar-thermal subsystem. For Configuration 1, the FPC array area required is 60 m^2, and the averaged flow rate per collector is 0.025 kg/s. For Configuration 2, the ETC array area is again 60 m^2, which is covered by 30 collectors connected in two-parallel branches, with a flow rate per collector of 0.025 kg/s.

6.2 Transient modelling of the overall system

On the basis of the results presented in Section 5 and considering the subsystem sizes resulting from the optimisation exercise (Section 6.1), one-day transient simulations (1-hour time steps) for three typical days (summer, autumn/spring and winter) are conducted in TRNSYS for a representative location in southern Europe (Athens, Greece). The simulations are conducted for both configurations considered in this work; the first based on FPCs and the second on ETCs. Fig. 7 shows the model, as defined in the TRNSYS environment, from which the power generated by the combined system is obtained under variable climate conditions. The schematic diagram in Fig. 7 corresponds to the FPC model configuration (it is noted that the diagram has been simplified for clarity). The corresponding diagram for the ETC model configuration is not shown but is similar. The main elements in both configuration are the solar thermal collector array, the hot water tank (thermal storage) and the ORC unit. In addition, the solar pump and controller unit are also shown.

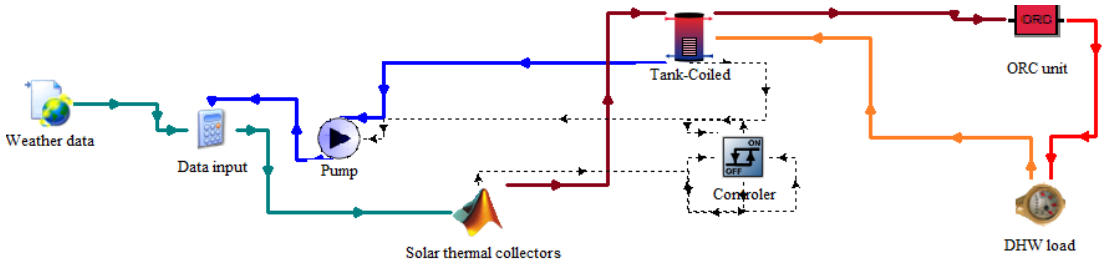

Fig. 7. Solar-ORC system model as defined and used in the TRNSYS environment for the transient simulations of the 3-D flat-plate collector array (here based on FPCs) and the ORC unit.

6.2.1 Configuration 1 – Flat-plate collector (FPC) array

Transient simulations are performed for Configuration 1 on three representative days, considering real weather data in TRNSYS with the ORC unit providing steady operation for 7 h/day (from 17:00 to 24:00). The following parameters are monitored: i) collector-array outlet temperature and fluid flow-rate; ii) solar irradiance; iii) auxiliary heating; iv) heat-source temperature and fluid flow rate to ORC; and v) outlet temperature from the ORC evaporator used to cover the domestic hot-water (DHW) load, amongst other. The evolution of selected parameters during the transient simulation are presented in Fig. 8a for an example autumn day. Similar plots are obtained when considering typical days in winter and summer, with the exception of lower/higher outlet temperatures from the collectors due to the different irradiance levels, corresponding to higher/lower auxiliary heating inputs, respectively.

Considering the representative days in summer, winter and autumn/spring as corresponding to 91, 90 and 184 days of the year, respectively, annual results can be extracted based on the simulations described above. The ORC engine using R245fa as the working fluid runs for 2,555 hours/year (29.1%) and generates 0.46 kW continuously when in operation, which leads to a total gross work output of 1,178 kWh/year. The auxiliary heating required is 72.8 kWh/year (99.8 W over a period of 2 h per day, on average). The total net work output from the combined FPC solar-ORC system is 1,105 kWh/year. In addition, the system supplies an equivalent of 10,710 $kW_{th}h$/year of DHW.

Further simulations were performed in which the operation (i.e. running hours) of the ORC engine were adjusted to coincide with the hours of solar availability. No significant differences in the total electrical and thermal outputs of the systems were found, mainly due to the efficient storage capability offered by the hot-water tank. This suggests that the operation of the solar-ORC system configuration integrated with TES can provide effective demand-side management (DSM) by offsetting the period of the ORC engine operation without significant deterioration in overall system performance.

6.2.2 Configuration 2 – Evacuated-tube collector (ETC) array

Transient simulations are also performed over the same three days for Configuration 2, in which the ORC engine is directly connected to the outlet of the ETC array, only running for the number of hours that the array outlet temperature is above 200 ºC. The heat-transfer fluid exiting the ORC evaporator is then used to provide further heating to the TES vessel, downstream of the ORC, before returning to the collector array (see Fig. 1b). The evolution of the selected system parameters are shown in Fig. 8b, for

comparison with the FPC system configuration in Fig. 8a. A similar approach is used to derive the annual performance from representative simulation days in summer, winter and autumn/spring.

For the ETC case, the ORC engine with R1233zd provides a continuous power output of 1.72 kW for a total operational period of 2,096 h/year, resulting in a gross annual work output from the combined solar-ORC system of 3,605.1 kWh/year. This corresponds to an annual solar-to-electrical conversion efficiency of 5.5%. In addition, the system supplies an equivalent of 13,175 $kW_{th}h$/year of DHW.

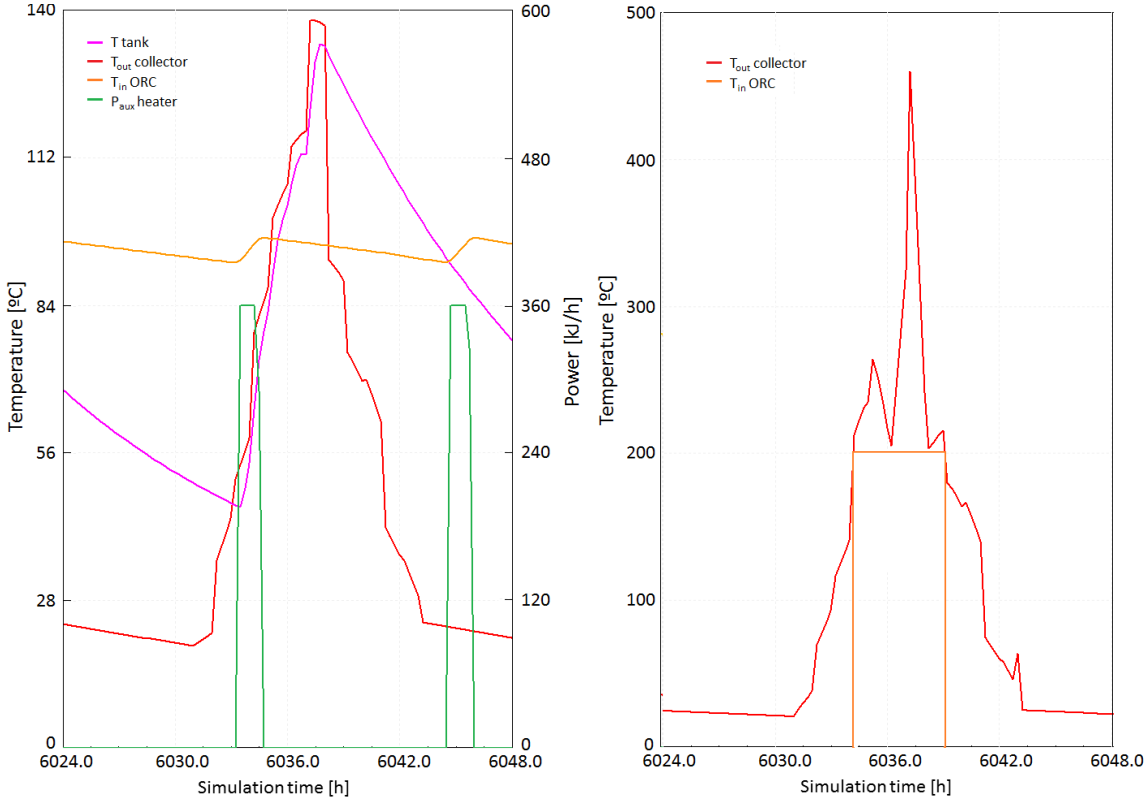

Fig. 8. Transient simulation of an autumn day in Athens for: (a) Configuration 1 and (b) Configuration 2.

The average domestic electrical power consumption in Greece is 0.44 kW (3,854 $kW_{el}h$/year) [24]. In the case of Configuration 1, this means that the solar-ORC system has the potential of covering about 31% of the annual domestic electricity demand, whereas Configuration 2 has the potential to cover 94% of the domestic electricity demand. At the same time, the average household DHW consumption in the south of Europe is around 2,100 $kW_{th}h$/year [13], such that Configurations 1 and 2 are capable of covering DHW demands of up to 5.0 and 6.3 households, respectively.

The results obtained from this present study can be extended with reasonable confidence to other southern regions in Europe (or elsewhere) with similar climatic conditions and solar resource. However, for locations with significantly different irradiance/weather conditions, a similar extensive system optimisation to that presented above should be performed for the particular location of interest.

7. Economic analysis and discussion

Based on the sizing results in Section 6, the capital cost for the alternative configurations is calculated. For the solar-thermal collectors and water tank, data from commercially available components have been used. For the ORC cost the costing techniques proposed by Turton [25] and Quoilin [26] have been used, because these are well-established methods found in the literature for ORC projects cost estimates [27], The cost correlations used for each system component are presented in Table 1.

The total investment cost for Configuration 1 (FPC-based system) amounts to 12,900 GBP, and for Configuration 2 (ETC-based system) it amounts to 22,490 GBP. Thus, the ETC configuration has a investment cost by approximately 70%, while generating ~3 times the power output. Considering the capital costs associated with the ORC subsystem components only, the specific investment costs (SICs) calculated for the FPC and ETC configurations amount to 7,900 GBP/kW and 3,500 GBP/kW,

respectively, mainly dominated by the higher power-output achieved in the latter. These figures fall within the middle-to-high end cost-range for small-scale ORC units (<5 kW) reported by Viking [31].

Table 1. Cost data used for the economic analysis

Component	Cost (GBP)	Ref.	Component	Cost (GBP)	Ref.
ORC evaporator (A, m^2)	$190 + 310A$	[26]	FPC (A, m^2)	$122A$	[28]
ORC condenser (A, m^2)	$190 + 310A$	[26]	ETC (A, m^2)	$261A$	[29]
ORC expander ($\dot{V}_{wf}$, lt/s)	$1.5(225 + 170\,\dot{V}_{wf})$	[26]	Thermal store (150 L)	964	[30]
ORC pump (W_p, kW)	$900(W_p/300)^{0.25}$	[26]	Controls	430	[25]
Cooling water pump (W_p, kW)	$900(W_p/300)^{0.25}$	[26]	Piping (l_p and d_p, m)	$(0.89 + 21d_p)l_p$	[26]
Solar fluid pump	387	[29]			

The cost breakdown for each configuration is presented in Fig. 9 for the best-performing ORC working fluids, in terms of power output achieved. For the FPC design and R245fa as the working fluid, the cost of the solar collectors amounts to more than 55% of the ORC investment cost, followed by the cost of the ORC expander, responsible for 8% of the total. For the ETC design with R1233zd as the working fluid, the cost of the solar collectors amounts for 65% of the total ORC cost, and the expander cost is responsible for 10% of the investment. Based on these results for both systems, it is concluded that the expander selection can significantly affect the cost of the ORC unit at low power outputs (<10 kW), whence these are bespoke components are associated in increased costs.

We now consider the *total* SIC (solar array plus ORC components) of the two configurations and compare them to a PV system with an approximate SIC of 1,150 GPB/kW$_{el}$ [33]. The total SIC of the FPC system configuration is 26,700 GBP/kW$_{el}$, whereas for the ETC configuration the SIC amounts to 2,035 GBP/kW$_{el}$. If one were to add the average thermal output (during operational hours) to the electrical output of the solar-ORC system in the calculation of the SIC, then the SIC is equal to 2,640 and 2,800 GBP/kW$_{(el+th)}$ for the FPC and ETC systems, respectively. It is noted that this approach overemphasises the value of the thermal output compared to the electrical output, however, it is important nonetheless that the economic value of the thermal output is not disregarded in the comparison against the PV system, which has no thermal output. It should also be noted that the thermal output of both solar-ORC configurations (and also the electrical output of the ETC-ORC configuration) is greater than that of a typical single-family household. Therefore, such systems can be installed in multiple-household residential applications (e.g. single apartment building with five flats) in which the initial investment cost could be shared among the individual households, with the solar-ORC system installed on a common roof area.

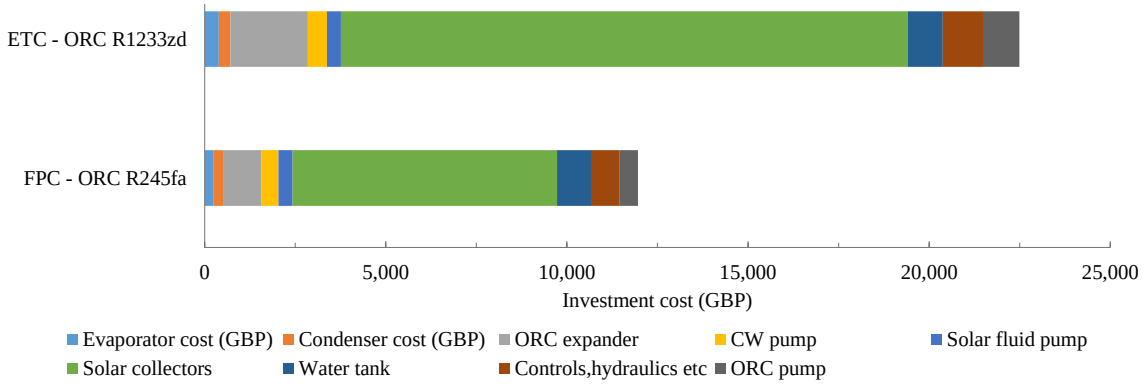

Fig. 9. Investment cost breakdown for Configuration 1 and Configuration 2 for the best performing fluids, in terms of power output.

8. Conclusions

Models have been developed of a high-efficiency solar-driven organic Rankine cycle (ORC) system for applications in the built environment. In particular, two different system configurations have been studied: 1) flat-plate collector-ORC (FPC-ORC) and 2) evacuated-tube collector-ORC (ETC-ORC). Firstly, it is evident that there is a need for optimising the ORC engine design to account for the

specific characteristics of the heat source and for the application constraints in general. Furthermore, in the limited literature considering solar-driven ORC units, the focus has been on the thermodynamic design of the ORC unit, rather than on the overall solar-ORC system optimisation. To address these observations, this work has focused on developing an optimisation model capable of maximising the electrical power output while also considering the operational constraints of the solar collector (temperature, flow-rate, etc.) in order to select the optimal array configuration for each collector type.

Secondly, the system optimisation performed for the selected location of Athens, Greece, resulted in significantly different results depending on the type of solar collector chosen. The best performing solar-ORC configuration when coupled with FPCs delivers a nominal net power output of 460 W, with R245fa as the working-fluid. The best performing system using ETCs generates power outputs exceeding 1,700 W, with R1233zd as working fluid. The difference in performance lies in the fact that ETCs are able to operate more efficiently at higher temperatures, and are also designed to operate with higher mass flow-rates than FPCs. These attributes result in an increased thermal input rate to the ORC unit at higher temperatures and pressures, generating more power and higher efficiencies.

From transient simulations of the optimised solar-ORC system configurations performed in TRNSYS, it is concluded that TES can provide effective DSM by offsetting the ORC operation period without a significant deterioration in the overall system performance. Finally, the higher power output of the ETC system comes at the cost of larger and more expensive system components. The total investment cost of the optimised solar-ORC with an FPC array amounts to 12,900 GBP, while the investment cost for an ORC coupled to an ETC array amounts to 22,400 GBP. The cost of the solar collectors and the expander are found to dominate the total investment cost. The specific investment cost of the proposed solar-ORC system is higher than that of domestic PV when only the electrical output is considered. However, a more sophisticated analysis is required in order to quantify the additional value of the thermal (hot water) output and also the DSM capability provided by the TES vessel, both of which are notable advantages compared to PV.

Acknowledgments

This work was supported by the UK Engineering and Physical Sciences Research Council (EPSRC) [grant numbers EP/M025012/1 and EP/J006041/1]. The authors would like to thank the Imperial College President's PhD Scholarship Scheme, and the Climate-KIC PhD Added Programme for funding this research. Data supporting this publication can be obtained on request from cep-lab@imperial.ac.uk.

References

[1] REN21 Secretariat. Renewables 2016 Global Status Report, 2016.

[2] Panwar N.L., Kaushik S.C., Surendra K., Role of renewable energy sources in environmental protection: a review. Renew Sustain Energy Rev., 2011, 1513-1524.

[3] International Energy Agency (IEA). Medium-Term Renewable Energy Market Report, 2016.

[4] Franz M., Werner W., Solar Heat Worldwide, 2015.

[5] EPIA, Solar Europe industry initiative, Implementation Plan 2010-2012, 2010.

[6] Philipps S.P., Bett A.W., Horowitz K., Kurtz S., Current status of concentrator photovoltaic (CPV) technology. 2016.

[7] Hoppmann J., Volland J., Schmidt T.S., Hoffmann V.H., The economic viability of battery storage for residential solar photovoltaic systems - A review and a simulation model. Renew. Sustain Energy Rev., 2014, 1101-1118.

[8] Freeman J., Hellgardt K., Markides C.N., An assessment of solar-powered organic Rankine cycle systems for combined heating and power in UK domestic applications. Appl. Energy, 2015, 605-620.

[9] Oyewunmi O., Markides C.N., Thermo-economic and heat transfer optimization of working-fluid mixtures in a low-temperature organic Rankine cycle system. Energies, 2016.

[10] Lecompte S., Huisseune H., van den Broek M., De Schampheleire S., De Paepe M., Part load based thermo-economic optimization of the organic Rankine cycle (ORC) applied to a combined heat and power (CHP) system. Appl. Energy, 2013, 871-881.

[11] Chatzopoulou M.A., Markides C.N., Modelling of advanced combined heat and power systems, ASTFE, 2017.

[12] Freeman J., Hellgardt K., Markides C.N., An assessment of solar-powered organic Rankine cycle systems for combined heating and power in UK domestic applications. Appl. Energy 2015, 605-620.

[13] Zangheri P., Armani R., Pietrobon M., Pagliano L., Heating and cooling energy demand and loads for building types in different countries of the EU. ENTRANZE Project, 2014.

[14] Himpe E., Janssens A., Rebollar J.E.V., Energy and comfort performance assessment of monitored low energy buildings connected to low-temperature district heating. Energy Procedia, 2015, 3465-3470.

[15] Klein S.A., TRNSYS 17: A Transient System Simulation Program, 2016.

[16] Guarracino I., Markides C.N., Mellor A., Ekins-Daukes N.J., Dynamic coupled thermal-and-electrical modelling of sheet-and-tube hybrid photovoltaic/thermal (PVT) collectors. Appl. Therm. Eng., 2016.

[17] Meteonorm: Irradiation data for every place on Earth. Available at: <http://www.meteonorm.com/> [accessed 23.1.2017].

[18] C1461 Solar Collector Factsheet Gasokol vacuTube 65/20. Available at: <http://www.spf.ch/fileadmin/daten/reportInterface/kollektoren/factsheets/scf1461en.pdf> [accessed 24.1.2017].

[19] Therminol® 66 Data sheet., Available at: <https://www.therminol.com/products/Therminol-66> [accessed 24.1.2017].

[20] Bergman T.L., Lavine A.S., Incropera F.P., DeWitt D.P., Fundamentals of Heat an Mass Transfer. John Wiley & Sons, 2011.

[21] Dobson M.K., Wattelet J.P., Chato J.C., Optimal Sizing of Two-Phase Heat Exchangers, 1993.

[22] Hewitt G.F., Shires G.L., Bott T.R., Process heat transfer. CRC Press, 1994.

[23] Shah M.M., A general correlation for heat transfer during film condensation inside pipes. Int. J. Heat Mass Transf., 1979, 547-556.

[24] Georghiou G.E., Existing Initiatives, Tariffs and PV Potential in Cyprus Promotion of PV energy through net metering optimization PV-NET: D3.1 - Existing initiatives, tariffs and PV potential in Cyprus, 2014.

[25] Turton R., Bailie R.C., Whiting W.B., Shaelwitz J.A., Analysis, Synthesis and Design of Chemical Processes. vol. 53. Third Edit. Pearson Education, 2009.

[26] Quoilin S., Declaye S., Tchanche B.F., Lemort V., Thermo-economic optimization of waste heat recovery organic Rankine cycles. Appl. Therm. Eng., 2011, 2885-2893.

[27] Lemmens S., Cost engineering techniques and their applicability for cost estimation of organic Rankine cycle systems. Energies, 2016.

[28] Flat Plate Collector Price 2017, Sulekha Solar. Available at: <http://www.sulekha.com/solar-water-heater/flat-plate-collector-solar-water-heater-prices-and-specifications> [accessed 20.1.2017].

[29] ORIGEN. Complete Pricelist. 2016. Available at: <http://www.origen.ie/v4/0940aa0c-5421-4a9b-840d-c9a2ae5d95bb/uploads/Origen_Price_Book.pdf> [accessed 20.1.2017].

[30] Herrando M., Markides C.N., Hybrid PV and solar-thermal systems for domestic heat and power provision in the UK: Techno-economic considerations. Appl. Energy, 2016, 512-532.

[31] Viking Heat Engines, 2016.

[32] Fraunhofer ISE, Levelized Cost of Electricity Renewable Energy Technologies, 2013.

[33] Kost J., Mayer J., Thomsen N., Hartmann C., Senkpiel S., Philipps S., Nold S., Lude N., Saad T., Schlegl C.N., Levelized Cost of Electricity Renewable Energy Technologies. 2013. Available at: <https://www.ise.fraunhofer.de/content/dam/ise/en/documents/publications/studies/Fraunhofer-ISE_LCOE_Renewable_Energy_technologies.pdf> [accessed 20.1.2017].